Colloids and Surfaces A 553 (2018) 368–377

Contents lists available at ScienceDirect

Colloids and Surfaces A

journal homepage: www.elsevier.com/locate/colsurfa

Solubilization of azo-dye-modified isatin derivative by amphiphilic carboxyresorcinarenes: The effect of macrocycle structure on the supramolecular association

Victor V. Syakaev[a,*], Julia E. Morozova[a,b], Andrei V. Bogdanov[a,b], Yana V. Shalaeva[a,b], Alina M. Ermakova[a,b], Alexandra D. Voloshina[a], Vladimir V. Zobov[a], Irek R. Nizameev[a,c], Marsil K. Kadirov[a], Vladimir F. Mironov[a,b], Alexander I. Konovalov[a]

[a] Arbuzov Institute of Organic and Physical Chemistry, FRC Kazan Scientific Center of RAS, Arbuzov str. 8, 420088 Kazan, Russian Federation
[b] Kazan Federal University, Kremlevskaya st. 18, 420008 Kazan, Russian Federation
[c] Kazan National Research Technical University named after A. N. Tupolev – KAI, K. Marx str. 10, 420111 Kazan, Russian Federation

GRAPHICAL ABSTRACT

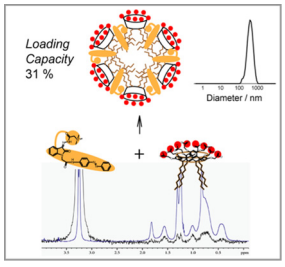

ARTICLE INFO

Keywords:
Isatin derivative
NMR spectroscopy
Resorcinarene
Solubilization
Supramolecular systems

ABSTRACT

Here we present the consecutive study of colloid systems formed by novel isatin derivative as compound with high pharmacological potential and series of carboxyresorcinarenes. The azo-modified isatin derivative bearing ammonium moiety (**I-3**) was synthesized and its antimicrobial activity was investigated. To increase its solubility the solubilization experiment using amphiphilic carboxyresorcinarenes, characterized by low hemolytic activity, was carried out. The **I-3** – macrocycles systems were studied by NMR, UV–vis, DLS and TEM. The FT PGSE and 2D NOESY NMR methods demonstrated, that solubilization of **I-3** is caused by the incorporation of its molecules in the hydrophobic part of the macrocycles associates. Herewith the loading efficiency of **I-3** into the macrocycles associates was reached of 20–30% due to the change of the volume of hydrophobic part of associates by varying the length and structure of hydrophobic substituents of macrocyclic amphiphiles.

1. Introduction

The growing demand on engineering of drug delivery systems promotes the new drug discovery and the development of the methods for improving their bioavailability. One of the ways to improve the solubility, biocompatibility, to reduce the toxicity and to preserve the premature biodegradation as well as for prolonged circulation in the body of hydrophobic drug is their non-covalent encapsulation in supramolecular associates of amphiphilic compounds such as liposomes [1], surfactants [2], polymers [3], and supramolecular macrocycles

* Corresponding author.
E-mail address: vsyakaev@iopc.ru (V.V. Syakaev).

https://doi.org/10.1016/j.colsurfa.2018.05.078
Received 14 March 2018; Received in revised form 24 May 2018; Accepted 27 May 2018
Available online 28 May 2018
0927-7757/

[4,5]. Recently, the ability of cyclodextrines [6,7] and cucurbit[n]urils [8] to form the inclusion complexes (endo-complexes) with hydrophobic drugs was reported. It was shown that such supramolecular association leads to the drug's solubility optimization and has the trigger-responsivity. Unlike them, amphiphilic calixarenes and resorcinarenes (amphiphiles with recognition sites [9]) demonstrate the loading ability of therapeutic compounds due to both the endo- and exo-complexes formation with substrates in co-associates [10–13]. This is due to their numerous sites to interact with substrate molecules: π-donor cavity, and upper- and lower-rim substituents with various functionalization. Herewith, the structure of amphiphilic resorcinarene influences on the way of the substrate inclusion in the co-associate, on its size, and the properties of the substrate in the co-associate [12].

The search of the new therapeutic compounds, caused by the resistance of many pathogens to previous generation drugs, the population growth, and the search for the low-cost pharmaceuticals, promotes the new drug discovery. It is known that isatin possesses the great potential since its heterocyclic scaffold has different functionalization sites and presents in a wide range of both synthetic and natural physiologically active compounds [14–20]. Among numerous isatin derivatives, the acylhydrazones, that exhibit antitumor [21–24], herbicidal [25], anti-tuberculosis [26] and other types of antimicrobial activity [27–33] attract special attention. In addition, a continuing interest in the application of isatin and its derivatives in the chemistry of functional materials [34–37] should be noted. At the other hand, some azo-compounds possess antibiotic, antifugal and anti-HIV properties [38]. Recently azo-derivatives of isatin have been obtained [39]. Despite the great synthetic and pharmaceutical potential of such hybrid compounds, their weak solubility in water is one of the disadvantages of their use as drugs. Therefore their solubilization in the colloid supramolecular systems can promote their usage as pharmaceuticals. Herewith the existence of the dynamic equilibrium in such systems and the possibility of the existence of different co-associates composition make it necessary to their preliminary study.

One of the methods that make it possible to understand the mechanism of interaction in supramolecular co-associates at the molecular level is NMR spectroscopy. Especially, Fourier transform pulsed-gradient spin—echo (FT-PGSE) NMR is a powerful and versatile tool to get knowledge on the structural behavior of all components in the supramolecular associate [40–45]. The self-diffusion coefficient (D_s) of a substrate molecule is related directly to its size and makes it possible to discern the free and bound molecules in the supramolecular system. That is why the FT-PGSE NMR method is widely and successfully used in the field of drug delivery supramolecular systems [45–47]. With the addition of 2D NOESY NMR data the information about specific structures of complexes between drug and binding site of supramolecular nanocontainers can be successfully obtained.

Here we represent the investigation of the solubilization of new azo-derivative of isatin by series of amphiphilic carboxyresorcinarenes. The study includes a few stages: i) the synthesis of new isatin derivative bearing azo-probe **I-3** and the study of the antimicrobial activity of **I-3** and its precursors; ii) the study of carboxyresorcinarenes hemotoxicity and their use as solubilizators for **I-3**, iv) the use of NMR spectroscopy methods for the investigation of the structure of **I-3** – macrocycles co-associates. The influence of different hydrophobicity of macrocycles on the macrocycle/**I-3** stoichiometry and on the composition of colloid solutions of **I-3** – macrocycles co-associates is discussed.

2. Experimental section

2.1. Materials and methods

Sodium dodecylsulfate (SDS), sodium bis-2-ethylhexyl sulphosuccinate (AOT) and sodium stearate were purchased from Aldrich, D_2O was purchased from Acros. CR, Cn-CR and C_5-N-CR were synthesised as reported previously [48,49]. Absorbance measurements were carried out on Lambda 35 UV/VIS Spectrometer (Perkin Elmer Instruments). DLS measurements were carried out on Zetasizer nano ZS (Malvern Instruments Ltd) equipped with a 4 mW He:Ne solid-state laser operating at 633 nm. Dispersion Technology Software 5.00 was used for the analysis of particle size. TEM images were obtained with Libra 120 (Carl Zeiss). The images were acquired at an accelerating voltage of 100 kV. Samples were dispersed on 300 mesh copper grids with continuous carbon-formvar support films.

2.2. Synthesis of 2-(2,3-Dioxoindolin-1-yl)-N-(4-(phenyldiazenyl)phenyl) acetamide (I-2)

To a magnetically stirred solution of isatin (**I-1**) (5 mmol) in dry DMF (15 ml) NaH (5 mmol, 60% suspension in mineral oil) was added in small portions at 10 °C. After 30 min to a dark violet reaction mixture 2-chloro-*N*-(4-(phenyldiazenyl)phenyl)acetamide (**Azo-CH_2Cl**) (5 mmol) was added followed by additional stirring at room temperature for 2 h. Then a solution was poured into a mixture of crushed ice/water (200 ml), the precipitate that formed was filtered off, washed consecutively with cold water (50 ml), ether (20 ml) and dried in vacuo (rt, 12 torr, 12 h). Orange powder were obtained (90 %), m.p.: 282–284 °C; ^{1}H NMR (600 MHz, DMSO-d_6): δ = 10.62 (s, 1H, NH), 7.91 (d, J = 8.8 Hz, 2H, Ar-H), 7.86 (d, J = 7.4 Hz, 2H, Ar-H), 7.82 (d, J = 8.8 Hz, 2H, Ar-H), 7.68 (t, J = 7.6 Hz, 1H, Ar-H), 7.63 (d, J = 7.4 Hz, 1H, Ar-H), 7.58 (m, 2H, Ar-H), 7.55 (d, J = 7.1 Hz, 1H, Ar-H), 7.20 (d, J = 7.6 Hz, 1H, Ar-H), 7.18 (d, J = 7.6 Hz, 1H, Ar-H), 4.65 (s, 2H, NCH_2). ^{13}C NMR (150 MHz, DMSO-d_6) 182.8 (C = O), 165.3 (C = O), 158.4 (C = O), 152.0 (CH), 150.8 (CH), 147.8 (CH), 141.3 (CH), 138.3 (CH), 131.1 (CH), 129.3 (CH), 124.5 (CH), 123.6 (CH), 123.5 (CH), 122.3 (CH), 119.7 (CH), 117.4 (CH), 111.0 (CH), 43.2 (CH_2). IR (ν, cm^{-1}, KBr) = 3310, 3135, 3070, 1743, 1719, 1681, 1614, 1597, 1549, 1472, 1409, 1302, 1252, 1153, 848, 754. MS (MALDI): 384 (M^+, 100). Found, %: C, 68.67; H, 4.10; N, 14.43. Calcd for $C_{22}H_{16}N_4O_3$, %: C, 68.74; H, 4.20; N, 14.58.

2.3. Synthesis of N,N,N-Trimethyl-2-oxo-2-(2-(2-oxo-1-(2-oxo-2-(4-(phenyldiazenyl)phenylamino)ethyl)indolin-3-ylidene)hydrazinyl) ethylammonium chloride (I-3)

To a mixture of compound (**I-2**) (5 mmol) and Girard's reagent T (5 mmol) in absolute ethanol (10 ml) at rt trifluoroacetic acid (3 drops) was added followed by refluxing for 3 h. After cooling to rt the precipitate was filtered off, washed with diethyl ether and dried in vacuum (18 torr) to give the corresponding product (**I-3**). Yellow powder (94 %), m.p.: 265–267 °C. ^{1}H NMR (500 MHz, DMSO-d_6): δ = 12.55 cis- and 12.94 trans- (s, 1H, NH-N), 10.96 (s, 1H, NHAr), 7.91 (d, J = 8.9 Hz, 2H, ArH), 7.86 (d, J = 8.4 Hz, 1H, ArH), 7.83 (d, J = 8.9 Hz, 2H, ArH), 7.69 (brd, J = 7.2 Hz, 1H, H4), 7.59 (t, J = 8.4 Hz, 1H, ArH), 7.54 (t, J = 8.4 Hz, 1H, ArH), 7.51 (t, J = 7.2 Hz, 1H, ArH), 7.25 (d, J = 7.2 Hz, 1H, ArH), 7.22 (t, J = 7.2 Hz, 1H, ArH), 4.68 (s, 2H, CHN), 4.57 trans- and 4.99 cis- (s, 2H, CHN^+), 3.34 (s, 9H, NH). ^{13}C NMR (DMSO-d_6, 126 MHz) δ = 166.2 (cis- C = O), 165.1 (C = O), 160.7 (C = O), 152.0 (CH), 147.8 (CH), 143.8 (C), 141.5 (C), 135.0 (C = N), 132.3 (CH), 131.1 (CH), 129.4 (CH), 123.7 (CH), 123.4 (CH), 122.3 (CH), 120.9 (CH), 119.5 (CH), 118.4 (C), 110.0 (CH), 63.1 trans- and 61.7 cis- (CH_2), 43.4 (CH_3), 42.9 (C-N). IR (ν, cm^{-1}, KBr) = 3428, 3213, 3171, 3026, 2948, 1694, 1618, 1599, 1541, 1498, 1474, 1380, 1301, 1254, 1154, 850, 695. MS (MALDI): 498 (M-Cl^+, 100). Found, %: C, 60.58; H, 5.19; Cl, 6.50; N, 18.20. Calcd for $C_{27}H_{28}ClN_7O_3$, %: C, 60.73; H, 5.28; Cl, 6.64; N, 18.36. Also see Figs. S1- S7.

2.4. Solubilization of I-3

The solubilization of **I-3** was performed in bidistilled water and D_2O is the presence and absence of macrocycles, surfactants and electrolytes by mixing at 25 °C for 5 h at a rate of 360 rpm. The solutions were centrifuged (rate 6 krpm, 10 min, centrifuge Eva-20 (Hettich

Zentrifugen, Germany)) to separate non-solubilized **I-3** and used in the next measurements. For determining of **I-3** concentration the aliquot of solution after centrifugation was diluted by EtOH (1/1 w/w) to prevent the influence of complexation on the absorbance intensity. Absorbance spectra of solutions were registered on quartz cell of 0.1 cm path length. The concentrations were defined with the help of calibration curve (Fig. S8). For the solutions with high absorbance intensity the appropriate dilution of solutions were used. The loading capacity (LC, %) of macrocycles or surfactant associates after solubilization of **I-3** were estimated by equation: $LC = 100\% \cdot C_{I\text{-}3}/(C_S + C_{I\text{-}3})$, where $C_{I\text{-}3}$ is concentration of **I-3** (mg/ml), C_S – concentration of macrocycle or surfactant (mg/ml).

2.5. NMR experiments

All NMR experiments were performed on a Bruker AVANCE(III)-500 spectrometer. The spectrometer was equipped with a Bruker multinuclear z-gradient inverse probe head capable of producing gradients with strength of 50 G cm^{-1}. All experiments were carried out at 303 ± 0.1 K. Chemical shifts were reported relative to HDO (4.7 ppm) as an internal standard. The Fourier transform pulsed-gradient spin-echo (FT-PGSE) experiments [42–44,50] were performed by BPP-STE-LED (bipolar pulse pair–stimulated echo–longitudinal eddy current delay) pulse sequence [51]. Data were acquired with a 50.0 ms diffusion delay, with bipolar gradient pulse duration from 2.2 to 6.0 ms (depending on the system under investigation), 1.1 ms spoil gradient pulse (30%) and a 5.0 ms eddy current delay. The bipolar pulse gradient strength was varied incrementally from 0.01 to 0.32 T/m in 16 steps. The temperature was set and controlled at 303 K with a 640 l/h airflow rate in order to avoid any temperature fluctuations owing to sample heating during the magnetic field pulse gradients. After Fourier transformation and baseline correction, the diffusion dimension was processed with the Bruker TopSpin software package (version 3.2). The diffusion constants were calculated by exponential fitting of the data belonging to individual columns of the pseudo 2D matrix. Single components have been assumed for the fitting routine. The diffusion experiments were preformed at least three times and only the data with the correlation coefficients of a natural logarithm of the normalized signal attenuation ($\ln I/I_0$) as a function of the gradient amplitude $b = \gamma^2\delta^2g^2(\Delta\text{-}\delta/3)$ (γ is the gyromagnetic ratio, g is the pulsed gradient strength, Δ is the time separation between the pulsed-gradients, δ is the duration of the pulse) higher than 0.999 were included. All separated peaks were analyzed and the average values were presented. The standard deviations of the self-diffusion coefficients determination did not exceed 5%. 2D NOESY experiments were performed with the mixing times of 50–400 ms with pulsed filtered gradient techniques.

The pulse programs for all NMR experiments were taken from the Bruker software library.

2.6. Study of antimicrobial activity of *I-1, I-2, I-3* and macrocycles - *I-3* associates

The antimicrobial activity of **I-1, I-2** and **I-3** were studied in vitro in concentration range of 500–0.97 μg/ml. The cultures used for testing included Gram-positive bacteria: *Staphylococcus aureus ATCC 209p*, *Bacillus cereus ATCC 8035*; *Gram-negative bacteria: Escherichia coli CDC F-50*, *Pseudomonas aeruginosa ATCC 9027*, and fungi: *Aspergillus niger BKMF-1119*, *Trichophyton mentagrophytes var. gypseum 1773*, and *Candida albicans 855–653*. The bacteriostatic and fungistatic properties were studied by a series of dilutions in liquid growth medium according to published procedures [52] to define the MIC as the minimal concentration of a compound that inhibits the growth of the corresponding test microorganism. The bactericidal and fungicidal activities were determined as described earlier [52].

2.7. Hemolysis of Human Red Blood Cells by macrocycles and macrocycles - *I-3* associates

The macrocycles were tested for their hemolytic activities against human red blood cells (hRBC) according to ref. [53]. Fresh hRBC with heparin was rinsed 3 times with 0.15 M NaCl by centrifugation for 10 min at 800 g and resuspended in 0.15 M NaCl. CR was dissolved in 0.15 M NaCl and added to 0.5 mL of a solution of the stock hRBC in 0.15 M NaCl to reach a final volume of 5 mL (final erythrocyte concentration, 10 % v/v). The resulting suspension was incubated under agitation for 1 h at 37 °C. The sample was centrifuged at 2000 g for 10 min. Release of hemoglobin was monitored by measuring the absorbance of the supernatant at 540 nm. Controls for zero hemolysis (blank) and 100% hemolysis consisted of hRBC suspended in 0.15 M NaCl and distilled water, respectively.

2.8. The preparation of macrocycle - *I-3* associates for antimicrobial and hemolytic activity study

To prepare the samples for antimicrobial activity tests the solubilization of **I-3** by 4 ml of aqueous solutions of C_8-CR (0.72 mM) and C_{11}-CR (1.17 mM) was performed as described in Section 2.4. The resulting concentrations of **I-3** were 0.407 mM (248 mg/ml) and 0.714 mM (381 mg/ml) in the solutions of C_8-CR and C_{11}-CR, respectively.

To prepare the samples for hemolytic activity tests the solubilization of **I-3** by aqueous solutions of C_5OPh-CR (10.16 mM, 8 ml), C_8-CR (8.68 mM, 8.25 ml) and C_{11}-CR (10.09 mM, 10 ml) was performed as described in Section 2.4. The resulting concentrations of **I-3** were 0.317, 0.155 mM and 0.647 mM in the solutions of C_5OPh-CR, C_8-CR and C_{11}-CR, respectively.

3. Results and discussion

3.1. Synthesis and antimicrobial activity of izatin derivatives

New azo-isatin compound **I-3** containing ammonium moiety was obtained in two steps (Fig. 1). At the first, the azo derivative **I-2** was obtained by alkylation of isatin sodium salt (obtained in situ from isatin **I-1** and sodium hydride) with the high yield. Then compound **I-3**, bearing azo-dye fragment, was obtained by acid-catalyzed reaction of substituted isatin **I-2** with Girard's reagent T. Assignment of signals in the NMR spectra of **I-3** was accomplished by means of 2D COSY, (^{1}H,^{13}C) HSQC and (^{1}H,^{13}C) HMBC experiments (Figs. S1-S5). The **I-3** molecule has hydrazone fragment, C(O)NH group of which can exist as *cis*- and *trans*-conformers, therefore the part of **I-3** spectral peaks is doubled. The analysis of ^{1}H NMR spectra demonstrates the existence of 75 % of *cis*- and of 25 % of *trans*-conformers of hydrazone C(O)NH group. The assignment to amide rotamers of the hydrazide fragment has been done according to the ideology described in our previous works [54,55].

The antimicrobial (bacteriostatic, fungistatic, bactericidal and fungicidal) activity of **I-1**, **I-2** and **I-3** compounds was studied in vitro (Table S1). Relative to the test microorganisms used, the starting isatin **I-1** does not possess antimicrobial activity, whereas compounds **I-2** and **I-3** exhibit antimicrobial activity against *Gram-positive bacteria S. aureus 209p* strains. Compound **I-3** show weak fungicidal activity against yeast-like fungus *C. albicans* in compare with reference drug ketoconazole. Herewith **I-3** is 4 times more active than reference drug chloroamphenicol against *S. aureus 209* and demonstrates the bactericidal activity against this strain. Thus, the antibacterial properties of **I-3** are improved in comparison with both starting isatin **I-1** and intermediate azo-compound **I-2**.

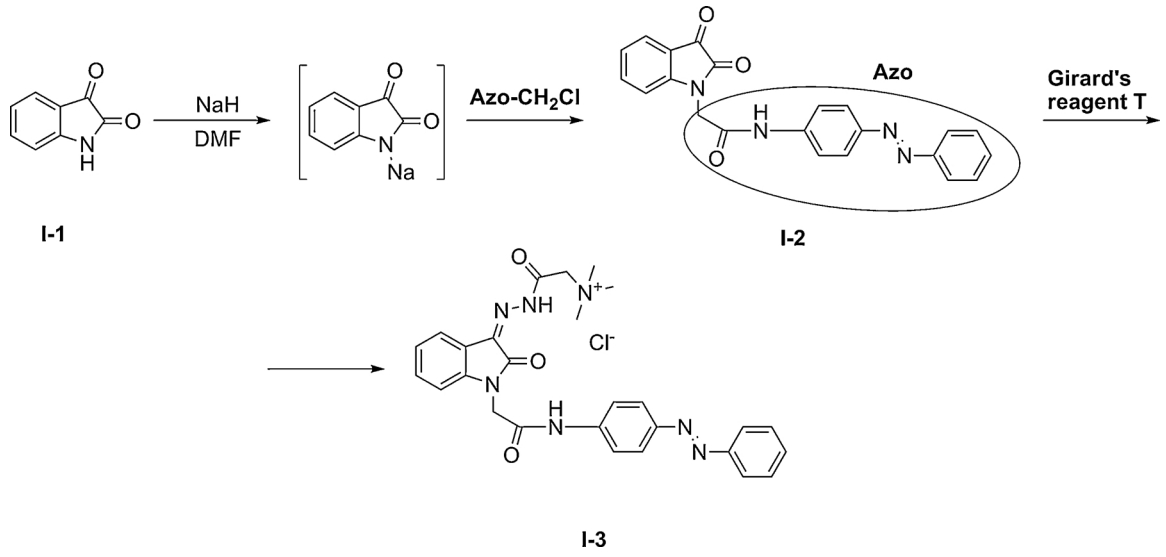

Fig. 1. Synthesis of acylhydrazone **I-3**.

*3.2. The hemolytic activity of carboxyresorcinarenes. The study of **I-3** solubilization by macrocycles with the help of UV-VIS, DLS and TEM methods*

The solubility of **I-3** in the bidistilled water is about 0.2 mM (UV-VIS method, Table 1). To improve its solubility the solubilization capacity of anionic resorcinarenes bearing eight (Cn-CR) and sixteen (C_5-N-CR) carboxy-groups on the upper rim was examined (Fig. 2). In the series of Cn-CR macrocycles the various hydrophobicity was provided by different lower rim substituents - pentyl (C_5-CR), octyl (C_8-CR), undecyl (C_{11}-CR), *p*-phenylene-oxy-pentyl (C_5OPh-CR), and *p*-phenylene-oxy-dodecyl (C_{12}OPh-CR). Earlier it was shown that in the aqueous solutions these macrocycles, which exist in the cone (C_5-CR, C_8-CR, C_{11}-CR) and boat conformation (C_5-N-CR, C_5OPh-CR, C_{12}OPh-CR), formed micelle-like self-associates, whose radius grows with the increase of the length of macrocycles lower rim substituents [48,49]. Therefore they can solubilize the poorly water-soluble compounds due to their incorporation into co-associates. Herewith the driving forces of the solubilization will be electrostatic, π-π, cation-π, CH-π interaction and hydrophobic effect.

Table 1
The solubilization data of **I-3** (UV-VIS and ^{1}H NMR methods); C_S and $C_{I\text{-}3}$ – the concentration of solubilizator and **I-3**, respectively, λ_{max} – the absorbance maximum of **I-3** in aqueous solutions.

S[a]	UV–vis				^{1}H NMR
	C_S, mM	λ_{max}, nm	$C_S/C_{I\text{-}3}$[b]	Loading capacity, %	$C_S/C_{I\text{-}3}$
C_5-CR	1	337	1/0.125	–	1/0.1
C_5OPh-CR	1	337	1/0.9	22.0	1/0.7
C_8-CR	1	339	1/1.3	31.1	1/1.1
C_{11}-CR	1	343	1/0.4	11.1	1/0.3
C_{12}OPh-CR	–	–	–	36.1[c]	1/2.3
C_5-N-CR	1	337	1/0.07	–	–
CR	4	338	1/0.08	–	1/0.06
H_2O	–	337	-/0.2	–	–
Borate buffer	–	331	-/[d]	–	–
HCl 0.1N	–	338	-/[d]	–	–
PBS pH 7	–	337	-/[d]	–	–
SDS	10	343	1/0.02	3.7	–
AOT	5	344	1/0.005	0.6	–
Stearate Na	1	337	1/0.08	12.4	–

[a] S - the solubilizator.
[b] $C_{I\text{-}3}$ values were estimated from UV VIS data after addition of EtOH to **I-3** aqueous solutions.
[c] from ^{1}H NMR data, C(C_{12}OPh-CR) 0.5 mM.
[d] trace.

The study of the macrocycles toxicity showed the low values of erythrocytes hemolysis in the solutions of macrocycles at 0.5 mM concentration with the exception of C_8-CR, whose toxicity is decreased with dilution (Table S2). The low hemotoxicity of carboxylic macrocycles is probably explained by the presence of anionic groups in the macrocycle molecules. Therefore, they can be used as supramolecular nanocontainers for solubilization of therapeutic compounds.

UV-VIS spectrum of **I-3** ethanol solution contains the absorption band with the maximum of 338 nm, which reflects the π-π* transition of azo-fragment (Fig. S9), so its solubilization into the aqueous solutions was estimated with the help of UV-VIS method. To determine the effect of the macrocycles structure on the solubilization, 1 mM aqueous solutions of macrocycles were used for solubilization of **I-3** as well as solutions of their monomer analog CR (4 mM, 4-fold excess is used in compare with macrocycles to simulate the conditions of a macrocyclic platform), anionic surfactants (SDS, AOT and sodium stearate in solutions with the concentrations above their cmc values), and electrolytes (0.1 N HCl, PBS pH 7.4, borate buffer pH 9.18). According to the UV-VIS data of obtained aqueous solutions of **I-3** (Fig. 3 and Table S3) the substrate practically is not soluble in the presence of electrolytes (0.1 N HCl, PBS pH 7.4, borate buffer pH 9.18), and is poorly solubilized in the aqueous solutions of AOT (5 mM), sodium stearate (1 mM), and macrocycles C_5-CR (1 mM) and C_5-N-CR (1 mM). The significant increase of **I-3** solubilization is observed in the C_5OPh-CR, C_8-CR, and C_{11}-CR macrocycle solutions (1 mM), and in the CR solution (4 mM). The poor solubility of **I-3** in the presence of electrolytes probably testifies its dependence on the ionic strength of solution. It is interesting, that among surfactants only SDS slightly increases solubility of substrate in the solution with concentration above cmc (Table S3). Herewith, the presence of anionic macrocycles in the solutions decreases (in the case of C_5-CR and C_5-N-CR) or increases (in the case of C_5OPh-CR, C_8-CR, and C_{11}-CR) the solubility of **I-3** in water. In the presence of macrocycles with longest hydrophobic groups - C_8-CR and C_{11}-CR, - and surfactants - SDS and AOT, – the absorbance maximum of **I-3** (λ_{max}) is batochromically shifted on 2 ÷ 7 nm in comparison with aqueous solution of substrate (Table 1). It indicates the preferred solubilization of substrate into the hydrophobic core of self-associates of these amphiphilic compounds, formed by their alkyl groups. In the solutions of macrocycles C_5-CR and C_5-N-CR their lower rim substituents are too small and unable to create the necessary microenvironment for

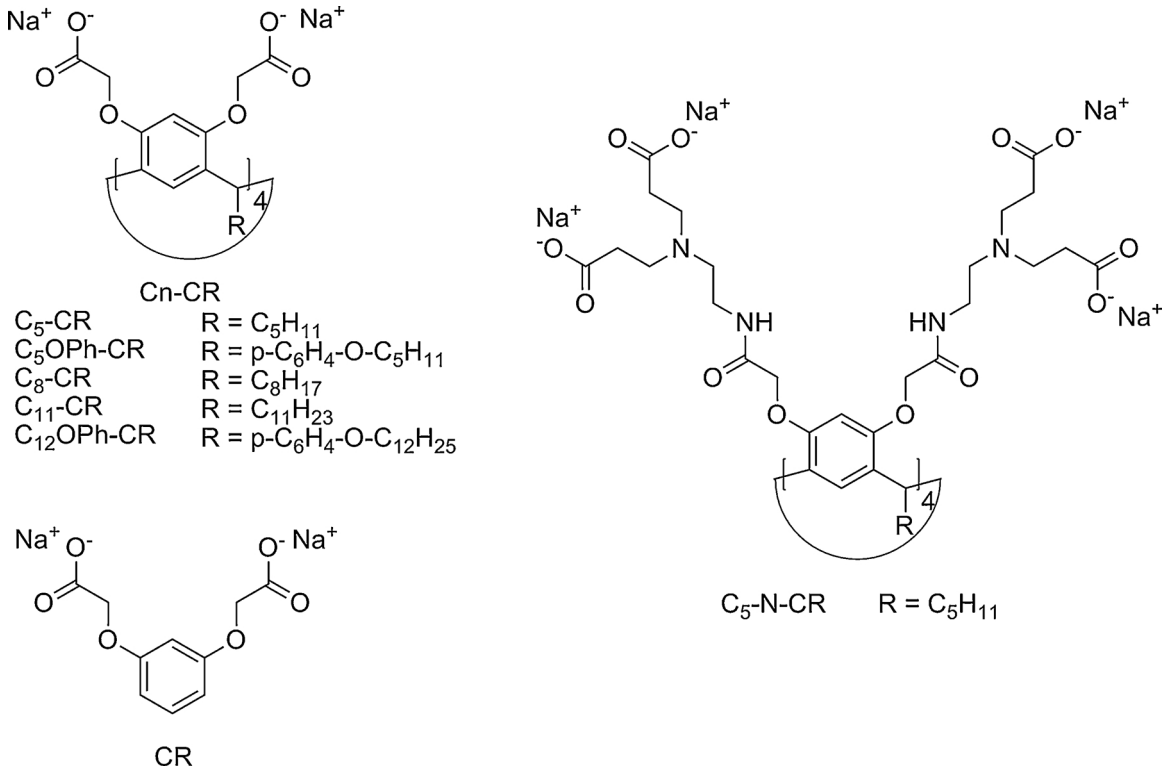

Fig. 2. The structure of carboxyresorcinarenes and their monomer analog.

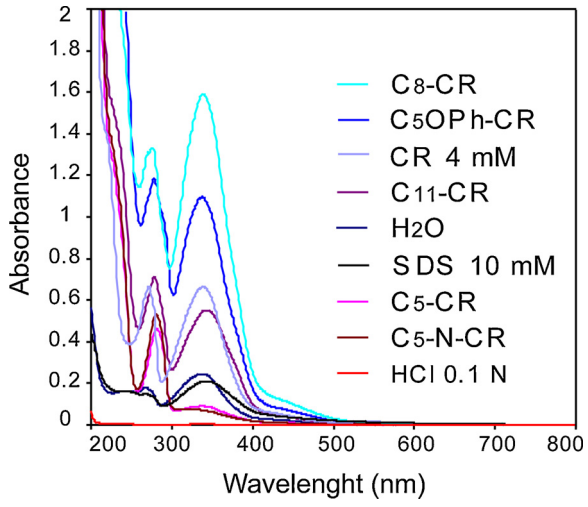

Fig. 3. UV-VIS spectra of **I-3** after solubilization in bidistilled water, 0.1 N HCl, aqueous solutions of macrocycles (1 mM), CR (4 mM) and SDS (10 mM) (quartz cell with 0.5 cm length, 15-fold dilution).

solubilization of the hydrophobic and bulk **I-3**. In the spectra of C_{11}-CR + **I-3** solution and SDS + **I-3** solution also the hypochromic shift of λ_{max}, i.e. the decrease of A^{max}, is observed (Fig. 3). Clearly, this is due to the influence of **I-3** complexation on its absorbance [56,57].

To prevent the influence of complexation on the dye absorbance intensity the determination of **I-3** concentration after solubilization was accomplished with the addition of ethanol to its aqueous solutions (H_2O/EtOH 1/1, λ_{max} of **I-3** is 340 nm) (Table S3). The addition of ethanol leads to the decrease of complexation strength and to the increase of substrate absorbance value ($A^{340\ nm}$). For example, in the aqueous solution the **I-3** absorbance in C_{11}-CR solution is less than in CR solution, and in the H_2O/EtOH 1/1 solution the **I-3** absorbance in C_{11}-CR solution is higher than in CR solution (Fig. 3, Table S3). The solubilization of **I-3** increases in the following row of H_2O ≈ SDS (10 mM) < CR (4 mM) < C_{11}-CR (1 mM) < C_5OPh-CR (1 mM) < C_8-CR (1 mM) (Table S3). On the base of obtained **I-3** concentrations the solubilizator/**I-3** molar ratio values and the loading capacity of associates have been also calculated (Table 1).

According to the data in Table 1 the solubilization of **I-3** is low in the presence of electrolytes and macrocycles bearing short alkyl substituents (C_5-CR and C_5-N-CR) and some anionic surfactants (AOT, sodium stearate). Compound CR consists of anonic groups and aromatic ring, it acts as hydrotrope [58] and increases the solubility of substrate better than SDS probably due to formation of ionic pair and π-π stacking with **I-3**. The increase of substrate solubility is observed in solutions of more hydrophobic C_5OPh-CR, C_8-CR and C_{11}-CR and can not be improved in solutions of more hydrophilic macrocycle by increasing of their concentration (on the example of C_5-CR, Fig. S10). Herewith it should be noted, that the substrate solubilization is not determined only by encapsulation into amphiphilic compounds self-associates, since the solubilizator/**I-3** molar ratio for C_5OPh-CR, C_8-CR and C_{11}-CR macrocycles is higher than for SDS (Table 1). For instance, the equimolar ratio of macrocycle/substrate is observed in the solution of C_5OPh-CR. And in the case of C_8-CR the macrocycle solubilizes more than 1 mole of **I-3**, while only light amount of substrate is solubilized in the surfactant solution (Table 1). As a result, the loading capacity of macrocycle associates of 10–30 % is achieved.

The highest loading capacity of **I-3** is found in C_5OPh-CR and C_8-CR co-associates (22 and 31 %, respectively). The increase of hydrophobicity in the co-associates of C_5OPh-CR and C_8-CR with **I-3** leads to the increase of hydrophobicity of supramolecular systems and their further aggregation into the large particles. As a result, their solutions are opalescent due to the presence of large particles with close size which confirmed by DLS and TEM methods (Fig. 4, Table S4).

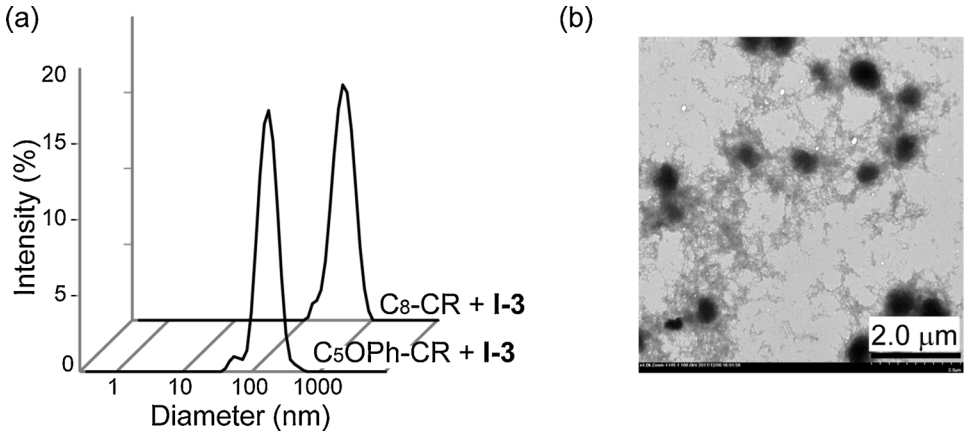

Fig. 4. (a) The intensity-averaged size distribution for C_5OPh-CR + **I-3** and C_8-CR + **I-3** solutions (DLS method, 25 °C, C(Cn-CR) 1 mM); (b) TEM images of C_8-CR + **I-3** (C(C_8-CR) = 0.5 mM; scale: b – 2 μm).

To determine the reasons of difference in the solubilization efficiency in macrocycles solutions and to speculate on the structure of the co-associates formed, NMR methods have been used.

*3.3. The study of Cn-CR + **I-3** co-associates by ^{1}H NMR, FT-PGSE NMR u 2D NOESY NMR methods*

According to ^{1}H NMR data the solubilization of **I-3** in the macrocycles solutions in D_2O leads to the upfield shift of $N(CH_3)_3^+$ signals of substrate in the spectra (to – 0.26 ppm, Table S5). Also in the spectra of **I-3** with C_{11}-CR and C_{12}OPh-CR the upfield shifts of signals of macrocycles alkyl substituents are observed (to -0.30 ppm, Table S5). Clearly, these changes should be associated with the closeness of $N(CH_3)_3^+$ group of **I-3** to aromatic fragments of macrocycles and of alkyl fragments of macrocycles to aromatic fragments of substrate. In the ^{1}H NMR spectra of **I-3** with C_8-CR and C_5OPh-CR two sets of aliphatic groups signals of macrocycles are observed, one of which has practically zeroed shift, and second has large upfield shift of signal (to -0.39 ppm, Table S5). Thus, there are two kinds of macrocycles molecules, present in these solutions, which interact with substrate differently. This conclusion is confirmed by FT-PGSE and 2D NOESY NMR data.

The NMR FT-PGSE method has shown, that in the spectra of CR + **I-3**, C_5-CR + **I-3**, C_{11}-CR + **I-3**, C_{12}OPh-CR + **I-3** solutions the one set of components signals is presented, and in the spectra of C_8-CR + **I-3** and C_5OPh-CR + **I-3** solutions two sets of signals of macrocycle and one set of substrate signals are presented (Table 2). In the CR (4 mM) + **I-3** solution the D_s of substrate slightly decreases (Table 2), but its concentration grows slightly in comparison with its individual solution (0.255 and 0.227 mM, respectively, Table S3) that testifies the interaction absence. In the C_5-CR + **I-3** solution the concentration of substrate is small, and D_s of macrocycle does not change. Probably, pentyl substituents of macrocycle are too short and macrocycle cannot organize the sufficient hydrophobic microenvironment for substrate solubilization, and the presence of ions in the C_5-CR solution hinders to **I-3** self-solubility in D_2O.

In solutions of macrocycles C_{11}-CR and C_{12}OPh-CR, which form the biggest self-associates among studied macrocycles, the solubilized substrate is practically completely bound ($P_b \sim 1$). In the 2D NOESY NMR spectra of C_{11}-CR + **I-3** and C_{12}OPh-CR + **I-3** solutions cross-peaks between signals of aromatic and NMe_3^+ groups of **I-3** and signals of macrocycles aliphatic groups are observed that confirmed the ^{1}H NMR data (Fig. 5). This testifies the incorporation of substrate molecules into the hydrophobic part of macrocycles associates, formed by their lower rim substituents.

In the presence of C_{11}-CR the solubility of **I-3** increases only slightly, probably, big self-associates of C_{11}-CR have a more dense charge on associates surface that decreases the chance of substrate penetration into the hydrophobic part of associates. 1 mol of C_{12}OPh-CR solubilizes 2.3 mol of **I-3**. Clearly, the solubilization increases due to the presence of oxy-phenylene groups in the macrocycle molecules. R_H values of co-associates of C_{11}-CR and C_{12}OPh-CR in the mixed solutions increase only for about 1.2-fold.

In the ^{1}H NMR and FT-PGSE NMR spectra of C_5OPh-CR + **I-3** and

Table 2
The FT-PGSE NMR data for **I-3** and Cn-CR in the individual and mixed solutions (D_2O, 303 K): D_s - the self-diffusion coefficient, P - the population of component in two exponential analyses of diffusion slope, R_H and N_{ag} – the experimental value of hydrodynamic radius and the aggregation number of macrocycle, respectively, P_b – the fraction of bound substrate. $C_{Cn\text{-}CR}$ = 1 mM.

	$C_{Cn\text{-}CR}/C_{I\text{-}3}$	$D_s \times 10^{-10}$, m^2/s		R_H[a], Å	N_{ag}	P_b
		I-3	Cn-CR			
I-3	–	4.24	–	–	–	–
CR[b]	–	–	5.68	4.9	–	–
CR[b] + **I-3**	1/0.06	4.13	5.65	4.9	–	0
C_5-CR	–	–	2.49	11.2	2.2	–
C_5-CR + **I-3**	1/0.1	[c]	2.50	11.1	2.1	–
C_{11}-CR	–	–	1.04	26.7	22	–
C_{11}-CR + **I-3**	1/0.3	0.86	0.86	32.2	39	1
C_{12}OPh-CR[d]	–	–	0.67	41.3	72	–
C_{12}OPh-CR[e] + **I-3**	1/2.3	0.72	0.56	49.4	123	0.96
C_5OPh-CR	–	–	2.06	13.5	2.7	–
C_5OPh-CR + **I-3**	1/0.7	0.85	2.12 (0.9)	13.1	1.4	–
			0.8 (0.1)	34.1	25	1
C_8-CR	–	–	1.85	15.0	4.5	–
C_8-CR + **I-3**	1/1.1	1.07	1.75 (0.3)	15.9	5.4	–
			1.10 (0.7)	26.1	23.6	1
C_8-CR + **I-3**	1/0.9[f]	1.10	1.75 (0.48)	15.9	5.4	–
			1.20 (0.52)	24.2	18.8	1
C_8-CR + **I-3**	1/0.4[f]	1.17	1.76 (0.65)	15.8	5.2	–
			1.20 (0.35)	23.9	18.2	1
C_8-CR + **I-3**	1/0.2[f]	1.37	1.82 (0.79)	15.3	4.7	–
			[g] (0.21)	[g]	[g]	–

[a] R_{Hteor} for C_5-CR is 8.6 Å, for C_8-CR is 9.1 Å, for C_{11}-CR is 9.5 Å, for C_5OPh-CR is 9.7 Å, for C_{12}OPh-CR is 9.9 Å, calculated with the help of HYDRONMR program [59].

[b] The concentration of CR is 4 mM.

[c] Impossible to estimate the D_s of **I-3** because of low concentration and the broadening of substrate signal caused by solubilization.

[d] The concentration of C_{12}OPh-CR is 0.1 mM.

[e] The concentration of C_{12}OPh-CR is 0.5 mM.

[f] Solutions are obtained by consequence dilution of C_8-CR + **I-3** (1/1.1) solution by 1 mM solution of C_8-CR.

[g] Impossible to estimate the D_s of macrocycle signals because of their broadening and T2* is too short.

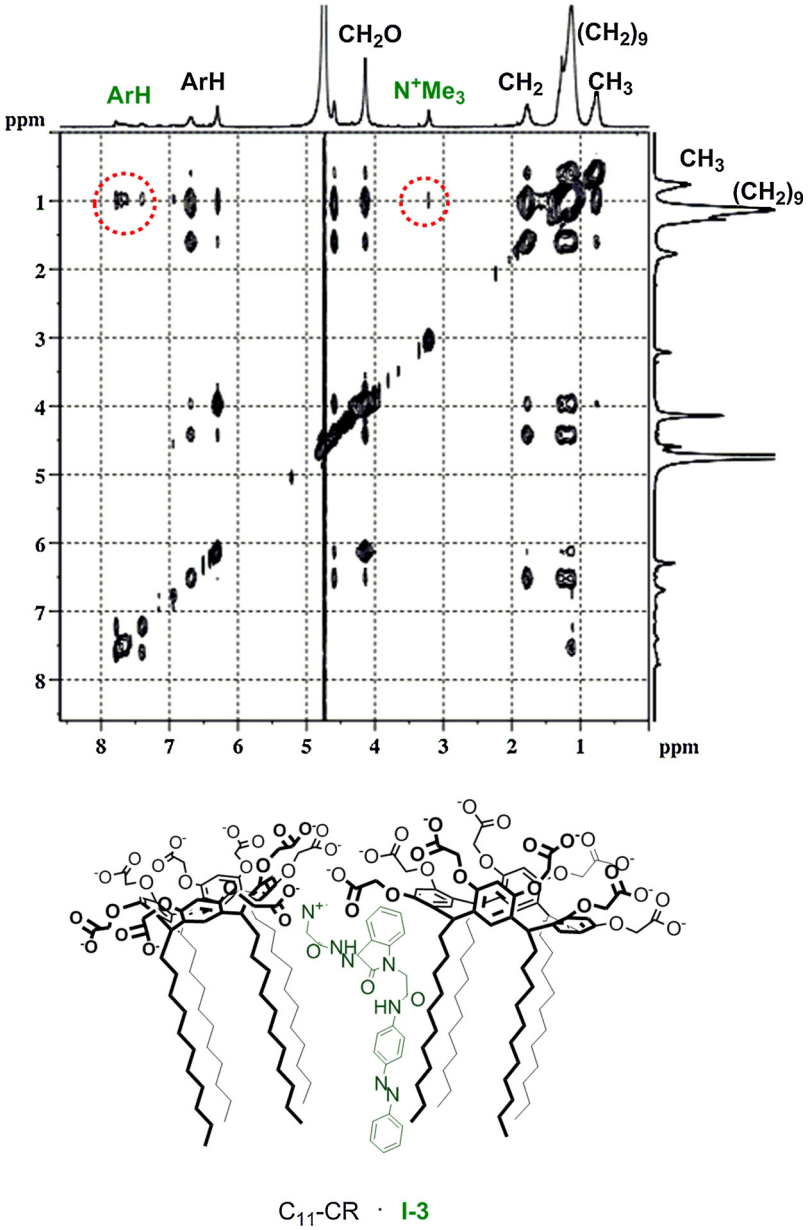

Fig. 5. 2D NOESY NMR spectra of C_{11}-CR + **I-3** and proposed scheme of their association.

C_8-CR + **I-3** two sets of macrocycles signals are observed. The part of C_5OPh-CR molecules with large upfield shifts of signals in the ^{1}H NMR spectra has the D_s value close to D_s of **I-3**. Herewith its population is about 10% and it strongly binds the substrate (P_b about 1). R_H value of co-associates increases of 2.5-fold, and DLS data suggest the presence of big particles in C_5OPh-CR + **I-3** solution (Fig. 4, Table S4). The difference in associates' sizes, obtained by FT-PGSE NMR and DLS methods is explained by the different fixing times of the particles in these methods. There are the order of $\sim 10^{-6}$ s in DLS and $\sim 10^{-2}$ s in FT-PGSE NMR.

Also in the case of C_8-CR + **I-3** solution the part of macrocycle molecules with upfield shifts in ^{1}H NMR spectra has D_s value close to D_s of substrate. To more detail characterization of C_8-CR + **I-3** interaction the solution with C_8-CR/**I-3** molar ratio of 1/1.1 was consequentially diluted by initial solution of C_8-CR and the series of solutions with different macrocycle/substrate molar ratio were obtained (Table 2). ^{1}H NMR spectra of all solutions also have two sets of macrocycles signals with greatest difference in the signals of aliphatic groups (Fig. 6). The analysis of FT-PGSE NMR spectra of solutions shows the different D_s

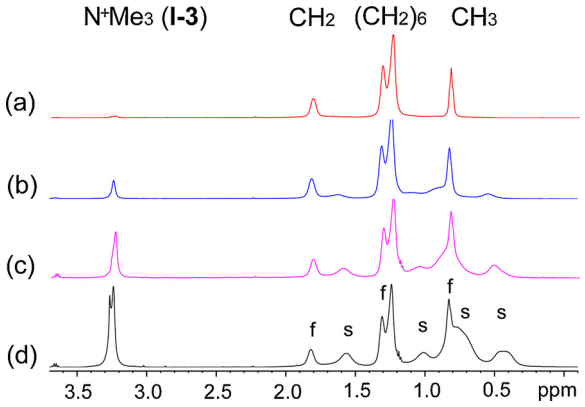

Fig. 6. The fragments of C_8-CR + **I-3** ^{1}H NMR spectra with different C_8-CR/**I-3** molar ratio (from bottom to top: 1/1.1, 1/0.9, 1/0.4, 1/0.2; the scale is changed for clarity).

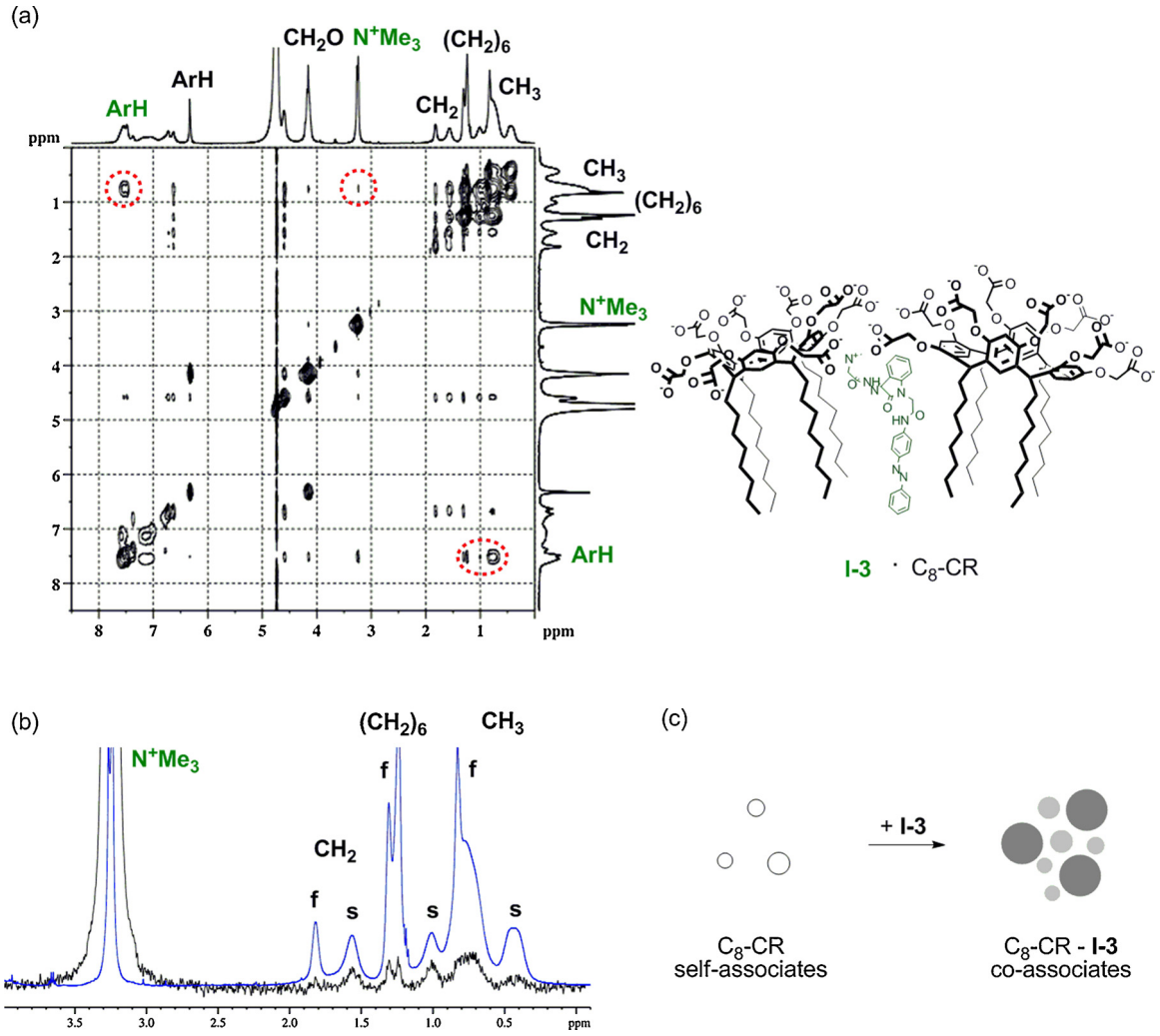

Fig. 7. a) 2D NOESY spectra of C_8-CR + **I-3** (C_8-CR/**I-3** molar ratio is 1/1.4, mixing time 400 ms) and the proposed scheme of C_8-CR - **I-3** association on the molecular level; b) The horizontal one-dimensional slices extracted from the 2D NOESY spectrum for signals of $N^+(CH_3)_3$ groups of **I-3** (***f*** and ***s*** – "fast" and "slow" parts of C_8-CR molecules, respectively; the scale is changed for clarity); c) The proposed scheme of C_8-CR - **I-3** association in supramolecular nanoparticles (the different colouring of circles reflects the different degree of substrate contents in macrocycle associates).

values for both sets of aliphatic groups' signals. For "fast" set D_s value is only slightly lower then D_s of macrocycle molecules in the individual solution, and in the ^{1}H NMR its signals shift insignificantly. At the same time D_s value of "slow" macrocycle molecules, the signals of which are shifted on 0.2-0.4 ppm in high fields, is close to D_s value of substrate. The large value of shifts of macrocycle aliphatic groups is caused by their proximity to aromatic fragments of **I-3**. This is also confirmed by the presence of cross-peaks between aromatic and $N(CH_3)_3^+$ fragments of **I-3** and aliphatic groups of "slow" part of macrocycle molecules in 2D NOESY NMR spectra (Fig. 7a). For clarity on Fig. 7c the horizontal one-dimensional slice is extracted from the 2D NOESY spectrum for signals of $N(CH_3)_3^+$ groups of **I-3** is shown, where the cross-peaks between this fragment of **I-3** with broadened signals of aliphatic groups are clearly visible.

In C_8-CR + **I-3** solutions with the decrease of the substrate concentration the integral intensity of upfield shifts set symbatically diminishes, i.e. the fraction of "slow" molecules, which interact with substrate, decreases. Herein, despite the dilution, average R_H value of C_8-CR + **I-3** associates always close to 2.4 – 2.3 nm. It can be assumed, that in the C_8-CR + **I-3** solutions the solubilization of substrate in the inner hydrophobic part of associates leads to the spontaneous accumulation nearby by these macrocycle molecules other substrate molecules with formation of co-associate, which has the deterministic size and the macrocycle/substrate stoichiometry. It is logical to suppose, that slight decrease of D_s of "fast" molecules relatively to the individual macrocycle solution means their interaction with C_8-CR + **I-3** associates (Fig. 7d). Such common association processes in the C_8-CR + **I-3** solution lead to the appearance of large particles, the existence of which are confirmed by DLS and TEM data (Fig. 4, Table S4).

Thus, in the C_8-CR + **I-3** solution and less in the C_5OPh-CR + **I-3** solution the macrocycle-substrate co-associates, which save their own stoichiometry and structure, and macrocycle self-associates, in contact with co-associates, exist. Apparently, in the case of C_8-CR and C_5OPh-CR the efficiency of solubilization is achieved by the correspondence of the sizes of hydrophobic part of macrocycles self-associates and the substrate, which allows **I-3** molecules to be in it, without impeding the electrostatic interaction of the head polar groups of macrocycle and substrate. Herein, the presence in C_5OPh-CR macrocycle hydrophobic substituents of oxy-phenylene groups in comparison with less bulky aliphatic chains in C_8-CR already lead to the solubilization decrease, that attests the enough fine-tuning of the co-association.

In total, the driving forces of **I-3** solubilization are electrostatic interaction with carboxy-groups of macrocycle and inclusion in the inner hydrophobic part of macrocyle associates due to the hydrophobic effect, CH-π, π-π and cation-π interactions. In the case of CR and C_5-CR the lack of enough hydrophobic microenvironment for **I-3** hinders its

effective interaction and solubilization. Large self-associates of C_{11}-CR are less permeable for substrate molecules due to tight surface charge, and in C_{12}OPh-CR self-associates this disadvantage is compensated by presence of oxy-phenylene groups in its lower rim substituents, which can bind substrate by addition π-π stacking. Finally, C_8-CR and C_5OPh-CR macrocycles form more comfortable conditions for **I-3** solubilization, which are realized due to it clusterization in the macrocycle-substrate co-associates and the formation of big co-associates with remaining macrocycles self-associates. The study of antibacterial activity of **I-3** in supramolecular associates showed that it does not increase in compare to pure **I-3** (Table S1). The hemolytic activity data of C_5OPh-CR – **I-3**, C_8-CR – **I-3**, and C_{11}-CR – **I-3** associates showed low values which are close to the values of macrocycles (Table S2). It can be concluded that formation of supramolecular associates does not significantly change the studied biological properties of their components.

4. Conclusions

Thus, novel azo-modified isatin derivative bearing ammonium moiety is synthesized and its solubilization by aqueous solutions of carboxyresorcinarenes of different hydrophobicity is studied. It has been shown that **I-3** has antimicrobial properties, and carboxyresorcinarenes are characterized by low hemolytic toxicity. The macrocycles self-associates solubilize the **I-3** with the incorporation of its molecules into the hydrophobic part of co-associates, formed by macrocycles lower rim substituents. Herewith the insignificant change of length and structure of hydrophobic groups of macrocycles leads to the acute increase of solubilization efficiency. The macrocycle/substrate stoichiometry in the co-associates was about 1/1 for macrocycle with octyl and pentyloxyphenylene groups and about 2/1 for macrocycle with dodecyloxyphenylene groups. In the case of C_5OPh-CR - **I-3** and C_8-CR - **I-3** co-associates the existence of exchange between particles with different substrate contents and the increase of system hydrophobicity leads to the formation of large supramolecular particles. The obtained results can be used in further understanding of the encapsulation of biologically active molecules for targeted drug delivery.

Appendix A. Supplementary data

Supplementary material related to this article can be found, in the online version, at doi:https://doi.org/10.1016/j.colsurfa.2018.05.078.

References

[1] Th.M. Allen, P.R. Cullis, Liposomal drug delivery systems: from concept to clinical applications, Adv. Drug Deliv. Rev. 65 (2013) 36–48.

[2] L. Zakharova, T. Pashirova, R. Kashapov, D. Gabdrakhmanov, O. Sinyashin, Drug delivery mediated by confined nanosystems: structure-activity relations and factors responsible for the efficacy of formulations, in: E. Andronescu, A.M. Grumezescu (Eds.), Nanostructures for Drug Delivery, Elsevier, 2017, pp. 749–806.

[3] Ch. Martin, N. Aibani, J.F. Callan, B. Callan, Recent advances in amphiphilic polymers for simultaneous delivery of hydrophobic and hydrophilic drugs, Ther. Deliv. 7 (2016) 15–31.

[4] M.J. Webber, R. Langer, Drug delivery by supramolecular design, Chem. Soc. Rev. 46 (2017) 6600–6620.

[5] L.Ya. Zakharova, R.R. Kashapov, T.N. Pashirova, A.B. Mirgorodskaya, O.G. Sinyashin, Self-assembly strategy for the design of soft nanocontainers with controlled properties, Mendeleev Commun. 26 (2016) 457–468.

[6] L. Tong, Y. Yang, X. Luan, J. Shen, X. Xin, Supramolecular hydrogels facilitated by α-cyclodextrin and silicone surfactants and their use for drug release, Colloids Surf. A 522 (2017) 470–476.

[7] R.R. Kashapov, V.A. Mamedov, N.A. Zhukova, M.K. Kadirov, I.R. Nizameev, L. Ya, O.G. Zakharova, Sinyashin, Controlling the binding of hydrophobic drugs with supramolecular assemblies of β-cyclodextrin, Colloids Surf., A 527 (2017) 55–62.

[8] E. Corda, M. Hernandez, S. Sanchez-Cortes, P. Sevilla, Cucurbit[n]urils (n = 6–8) used as host molecules on supramolecular complexes formed with two different drugs: emodin and indomethacin, Colloids Surf. A (2018), http://dx.doi.org/10.1016/j.colsurfa.2018.04.068.

[9] S. Shinkai, S. Mori, H. Koreishi, T. Tsubaki, O. Manabe, Hexasulfonated calix[6]arene derivatives: a new class of catalysts, surfactants, and host molecules, J. Am. Chem. Soc. 108 (1986) 2409–2416.

[10] Z. Qin, D.-S. Guo, X.-N. Gao, Y. Liu, Supra-amphiphilic aggregates formed by p-sulfonatocalix[4]arenes and the antipsychotic drug chlorpromazine, Soft Matter 10 (2014) 2253–2263.

[11] Y.-X. Wang, D.-Sh. Guo, Y.-Ch. Duan, Y.-J. Wang, Y. Liu, Amphiphilic p-sulfonatocalix[4]arene as "drug chaperone" for escorting anticancer drugs, Sci. Rep. 5 (2015) 9019.

[12] Ju.E. Morozova, V.V. Syakaev, E.Kh. Kazakova, Ya.V. Shalaeva, I.R. Nizameev, M.K. Kadirov, A.D. Voloshina, V.V. Zobov, A.I. Konovalov, Amphiphilic calixresorcinarene associates as effective solubilizing agents for hydrophobic organic acids: construction of nano-aggregates, Soft Matter 12 (2016) 5590–5599.

[13] C.M.A. Gangemi, A. Pappalardo, G.T. Sfrazzetto, Applications of supramolecular capsules derived from resorcin[4]arenes, calix[n]arenes and metallo-ligands: from biology to catalysis, RSC Adv. 64 (2015) 51919–51933.

[14] S.N. Pandeya, S. Smitha, M. Jyoti, S.K. Sridhar, Biological activities of isatin and its derivatives, Acta Pharm. 55 (2005) 27–46.

[15] K.L. Vine, L. Matesic, Ju.M. Locke, D. Skropeta, Recent highlights in the development of isatin-based anticancer agents, in: M. Prudhomme (Ed.), Advances in Anticancer Agents in Medicinal Chemistry, Bentham Science, 2013, pp. 254–312.

[16] P. Saraswat, G. Jeyabalan, M.Z. Hassan, M.U. Rahman, N.K. Nyola, Review of synthesis and various biological activities of spiro heterocyclic compounds comprising oxindole and pyrrolidine moities, Synth. Commun. 46 (2016) 1643–1664.

[17] G.S. Singh, Z.Y. Desta, Isatins as privileged molecules in design and synthesis of spiro-fused cyclic frameworks, Chem. Rev. 112 (2012) 6104–6155.

[18] P. Limpachayaporn, M. Schafers, G. Haufe, Isatin sulfonamides: potent caspases-3 and -7 inhibitors, and promising PET and SPECT radiotracers for apoptosis imaging, Future Med. Chem. 7 (2015) 1173–1196.

[19] A. Medvedev, O. Buneeva, O. Gnedenko, P. Ershov, A. Ivanov, Isatin, an endogenous nonpeptide biofactor: a review of its molecular targets, mechanisms of actions, and their biomedical implications, BioFactors (2018), http://dx.doi.org/10.1002/biof.1408.

[20] A.V. Bogdanov, V.F. Mironov, Synthesis of isatoic anhydride derivatives, Chem. Heterocycl. Compd. 52 (2016) 90–92.

[21] H.S. Ibrahim, S.M. Abou-Seri, M. Tanc, M.M. Elaasser, H.A. Abdel-Aziz, C.T. Supuran, Isatin-pyrazole benzenesulfonamide hybrids potently inhibit tumor-associated carbonic anhydrase isoforms IX and XII, Eur. J. Med. Chem. 103 (2015) 583–593.

[22] A. Gürsoy, N. Karali, Synthesis and primary cytotoxicity evaluation of 3-[[(3-phenyl-4(3H)-quinazolinone-2-yl)mercaptoacetyl]hydrazono]-1H-2-indolinones, Eur. J. Med. Chem. 38 (2003) 633–643.

[23] A. Karpenko, M. Shibinskaya, N. Zholobak, Z. Olevinskaya, S. Lyakhov, L. Litvinova, M.Y. Spivak, S. Andronati, Synthesis, DNA-binding, and interferon-inducing properties of isatin and benzoisatin hydrazones, Pharm. Chem. J. 40 (2006) 595–602.

[24] J.J. Gui, M. McTigue, M. Nambu, M. Tran-Dubé, M. Pairish, H. Shen, L. Jia, H. Cheng, J. Hoffman, P. Le, M. Jalaie, G.H. Goetz, K. Ryan, N. Grodsky, Y. Deng, M. Parker, S. Timofeevski, B.W. Murray, Sh. Yamazaki, Sh. Aguirre, Q. Li, H. Zou, J. Christensen, Discovery of a novel class of exquisitely selective mesenchymal-epithelial transition factor (c-MET) protein kinase inhibitors and identification of the clinical candidate 2-(4-(1-(quinolin-6-ylmethyl)-1H-[1,2,3]triazolo[4,5-b]pyrazin-6-yl)-1H-pyrazol-1-yl)ethanol (PF-04217903) for the treatment of cancer, J. Med. Chem. 55 (2012) 8091–8109.

[25] J. Wang, H. Tan, Y. Li, Y. Ma, Zh. Li, L.W. Guddat, Chemical synthesis, in vitro acetohydroxyacid synthase (AHAS) inhibition, herbicidal activity, and computational studies of isatin derivatives, J. Agric. Food Chem. 59 (2011) 9892–9900.

[26] T. Aboul-Fadl, F.A.S. Bin-Jubair, O. Aboul-Wafa, Schiff bases of indoline-2,3-dione (isatin) derivatives and nalidixic acid carbohydrazide, synthesis, antitubercular activity and pharmacophoric model building, Eur. J. Med. Chem. 45 (2010) 4578–4586.

[27] F.H. Havaldar, A.R. Patil, Syntheses of some novel [4-(4-oxo-2-phenyl-4h-quinazolin-3-yl)-phenoxy]-acetic acid [1-substituted aminomethyl-2-oxo-1,2-dihydro-indol-3-ylidene]-hydrazide derivatives and their potential biological activity, Heterocycl. Commun. 14 (2008) 107–114.

[28] S.N. Kanchana, V. Burra, L.K.R. Nath, Novel synthesis and anti-microbial activity study of innovative Mannich bases containing 2-phenoxy-1, 3, 2-dioxa phospholanes and indole systems, Orient. J. Chem. 30 (2014) 1349–1360.

[29] A.A. Radwan, Design, synthesis and molecular modelling of novel 4-thiazolidinones of potential activity against gram positive bacteria, Med. Chem. Res. 22 (2013) 1131–1141.

[30] A.V. Bogdanov, T.A. Kutuzova, D.B. Krivolapov, A.B. Dobrynin, V.F. Mironov, 1-Chloroacetyloxindole(isatin) in reactions with some N-nucleophiles. Unexpetedly easy cleavage of chloroacetyl group, Russ. J. Gen. Chem. 86 (2016) 539–543.

[31] A.V. Bogdanov, A.B. Kutuzova, V.F. Mironov, First examples of isatin acylhydrazones with ammonium fragment, Russ. J. Gen. Chem. 86 (2016) 756–757.

[32] A.V. Bogdanov, I.F. Zaripova, A.D. Voloshina, A.S. Strobykina, N.V. Kulik, S.V. Bukharov, Ju.K. Voronina, A.R. Khamatgalimov, V.F. Mironov, Synthesis and antimicrobial activity evaluation of some novel water-soluble isatin-3-acylhydrazones, Monatsh. Chem. 149 (2018) 111–117.

[33] A.V. Bogdanov, I.F. Zaripova, A.D. Voloshina, A.S. Strobykina, N.V. Kulik, S.V. Bukharov, V.F. Mironov, Isatin derivatives containing sterically hindered phenolic fragment and water-soluble acyl hydrazones on their basis: synthesis and antimicrobial activity, Russ. J. Gen. Chem. 88 (2018) 57–67.

[34] E.D. Głowacki, G. Voss, N.S. Sariciftci, 25th anniversary article: progress in chemistry and applications of functional indigos for organic electronics, Adv. Mater. 25 (2013) 6783–6800.

[35] A.V. Bogdanov, L.I. Musin, V.F. Mironov, Advances in the synthesis and application of isoindigo derivatives, Arkivoc vi (2015) 362–392.

[36] Sh. Li, J. Yuan, P. Deng, W. Ma, Q. Zhang, Synthesis and photovoltaic properties of

new conjugated polymers based on two angular-shaped naphthodifuran isomers and isoindigo, Sol. Energy Mater. Sol. Cells 118 (2013) 22–29.
[37] T. Lei, J.-Y. Wang, J. Pei, Design, synthesis, and structure–property relationships of isoindigo-based conjugated polymers, Acc. Chem. Res. 47 (2014) 1117–1126.
[38] E. Węglarz-Tomczak, Ł. Górecki, Azo dyes – biological activity and synthetic strategy, Chemik 66 (2012) 1298–1307.
[39] L.I. Musin, I.T. Abdullin, A.E. Vandyukov, D.G. Yakhvarov, R.G. Zinnatullin, V.F. Mironov, A.V. Bogdanov, Novel azo-dyes-modified isatin derivatives: synthesis, UV/VIS spectroscopic, and electrochemical study, Helv. Chim. Acta 99 (2016) 597–600.
[40] Y.-J. Schneider, A.K. Yatsimirsky, Principles and Methods in Supramolecular Chemistry, John Wiley & Sons, New York, 2000.
[41] I. Furo, NMR spectroscopy of micelles and related systems, J. Mol. Liq. 117 (2005) 117–137.
[42] P. Stilbs, Fourier transform pulsed-gradient spin-echo studies of molecular diffusion, Prog. Nucl. Magn. Reson. Spectrosc. 19 (1987) 1–45.
[43] Y. Cohen, L. Avram, L. Frish, Diffusion NMR spectroscopy in supramolecular and combinatorial chemistry: an old parameter - new insights, Angew. Chem. Int. Ed. Engl. 44 (2005) 520–554.
[44] E.J. Brand, S. Cabrita, S. Berger, Intermolecular interaction as investigated by NOE and diffusion studies, Prog. Nucl. Magn. Reson. Spectrosc. 46 (2005) 159–196.
[45] K.I. Momot, Ph.W. Kuchel, Pulsed field gradient nuclear magnetic resonance as a tool for studying drug delivery systems, Concepts Magn. Reson. Part A 19 A (2003) 51–64.
[46] A.R. Bilia, M.C. Bergonzi, F.F. Vincieri, P. Lo Nostro, G.A. Morris, A diffusion-ordered NMR spectroscopy study of the solubilization of artemisinin by octanoyl-6-O-ascorbic acid micelles, J. Pharm. Sci. 91 (2002) 2265–2270.
[47] M.L. Sommerville, C.S. Johnson Jr., J.B. Cain, F. Rypacek, A.J. Hickey, Lecithin microemulsions in dimethyl ether and propane for the generation of pharmaceutical aerosols containing polar solutes, Pharm. Dev. Technol. 7 (2002) 273–288.
[48] D. Mironova, L. Muslinkina, V. Syakaev, Ju. Morozova, V. Yanilkin, A. Konovalov, E. Kazakova, Crystal violet dye in complexes with amphiphilic anionic calix[4]resorcinarenes: binding by aggregates and individual molecules, J. Colloid Interface Sci. 407 (2013) 148–154.
[49] A.M. Ermakova, J.E. Morozova, Y.V. Shalaeva, V.V. Syakaev, I.R. Nizameev, M.K. Kadirov, I.S. Antipin, A.I. Konovalov, Calixresorcinarene-capped silver nanoparticles as new supramolecular hybrid nanocontainers, Mendeleev Commun. 27 (2017) 335–337.
[50] C.S. Johnson Jr., Diffusion ordered nuclear magnetic resonance spectroscopy: principles and applications, Prog. Nucl. Magn. Reson. Spectrosc. 34 (1999) 203–256.
[51] D. Wu, A. Chen, C.S. Johnson Jr., An improved diffusion-ordered spectroscopy experiment incorporating bipolar-gradient pulses, J. Magn. Reson. 115 (1995) 260–264.
[52] V.E. Semenov, A.D. Voloshina, N.V. Kulik, A.S. Strobykina, R.Kh. Giniyatullin, L.F. Saifina, A.E. Nikolaev, E.S. Krylova, V.V. Zobov, V.S. Reznik, Macrocyclic and acyclic 1,3-bis[5-(trialkylammonio)pentyl]-5(6)-substituted uracil dibromides: synthesis, antimicrobial properties, and the structure—Activity relationship, Russ. Chem. Bull. 64 (2015) 2885–2896.
[53] A.D. Voloshina, V.E. Semenov, A.S. Strobykina, N.V. Kulik, E.S. Krylova, V.V. Zobov, V.S. Reznik, Synthesis and antimicrobial and toxic properties of novel 1,3-bis(alkyl)-6-methyluracil derivatives containing 1,2,3- and 1,2,4-triazolium fragments, Russ. J. Bioorg. Chem. 43 (2017) 170–176.
[54] V.V. Syakaev, S.N. Podyachev, B.I. Buzykin, Sh.K. Latypov, V.D. Habicher, A.I. Konovalov, NMR study of conformation and isomerization of aryl- and heteroarylaldehyde 4-tert-butylphenoxyacetylhydrazones, J. Mol. Struct. 788 (2006) 55–62.
[55] V.V. Syakaev, S.N. Podyachev, A.T. Gubaidullin, S.N. Sudakova, A.I. Konovalov, The conformation and dynamic behaviour of tetrathiacalix[4]arenes functionalized by hydrazide and hydrazone groups, J. Mol. Struct. 885 (2008) 111–121.
[56] P. Thordarson, Determining association constants from titration experiments in supramolecular chemistry, Chem. Soc. Rev. 40 (2011) 1305–1323.
[57] N.O. Mchedlov-Petrossyan, L.N. Vilkova, N.A. Vodolazkaya, A.G. Yakubovskaya, R.V. Rodik, V.I. Boyko, V.I. Kalchenko, The nature of aqueous solutions of a cationic calix[4]arene: a comparative study of dye–calixarene and dye–surfactant interactions, Sensors 6 (2006) 962–977.
[58] V. Dhapte, P. Mehta, Advances in hydrotropic solutions: an updated review, St. Petersb. Polytech. Univ. J.: Phys. Math. 1 (2015) 424–435.
[59] J.G. de la Torre, M.L. Huertas, B. Carrasco, HYDRONMR: prediction of NMR relaxation of globular proteins from atomic-level structures and hydrodynamic calculations, J. Magn. Reson. 147 (2000) 138–146.